Late Quaternary deposition of ice-rafted sand in the subpolar North Atlantic (lat 40° to 65°N)

WILLIAM F. RUDDIMAN *Lamont-Doherty Geological Observatory, Palisades, New York 10964*

ABSTRACT

A major change in the North Atlantic pattern of ice-rafting deposition, during the last interglacial-glacial cycle, occurred approximately 75,000 B.P. Prior to this time, deposition for a period of almost 50,000 yr during isotopic stage 5 was greatest in the northwest near Greenland and Newfoundland. The main glacial pattern was very different; the main depositional axis shifted abruptly to a zonal axis along lat 46° to 50°N, reflecting the passage of ice farther from the pole before reaching water warm enough in which to melt. This pattern remained essentially unchanged for 65,000 yr during the main Würm glaciation.

The peak interglacial depositional pattern can best be explained by analogy with the modern oceanic flow, except for the addition of a concentrated eastward component along lat 50°N. The glacial pattern is also best explained by counterclockwise flow. Laurentide and Greenlandic ice entering the western North Atlantic from the Labrador Sea moved to the east and southeast directly into the glacial depositional maximum. Scandinavian ice dropped part of its bed load near Norway, looped to the southwest into the North Atlantic in a counterclockwise passage south of Iceland, and finally melted along the primary depositional maximum.

Total input rates of ice-rafted sediment to the Atlantic and Norwegian Sea increased slightly at 115,000 B.P. (the glacial inception), rose markedly at 75,000 B.P. (the major glacial transition), and continued to rise late in the Würm toward the late-glacial maximum. North Atlantic ice-rafting deposition is thus positively correlated with ice-sheet size.

During Quaternary time, roughly 70% of ice-rafted deposition of continental detritus in the world's oceans has occurred in the subpolar North Atlantic south of Iceland. During the past 3 m.y., a mass of wet unconsolidated drift estimated at 200,000 km^3 has been moved from the continents to the deep Atlantic by ice-rafting alone. This is equivalent to a layer of drift 16 m thick over all parts of the continents thought to have supplied ice-rafted detritus to the North Atlantic.

INTRODUCTION

Ice-rafted detritus is a product of the land, ice, and water realms. Its absolute input in space and time basically defines when, where, and at what rates sediment is dropped from melting ice during passage from land to subpolar oceans. Ice-rafted input may also point to changes both in oceanic circulation and in the size of ice sheets on land.

This study utilizes 32 cores indicating high deposition rates from the subpolar North Atlantic Ocean; the cores are fixed in time by excellent stratigraphic control and were sampled at average intervals of 3,000 yr. The study focuses on a sediment fraction that, judging by size (>62 μm) and nongraded dissemination within the cores, can only be an ice-rafted product. The absolute input of ice-rafted sand is determined for seven intervals of late Quaternary time, beginning with the start of the last interglaciation and ending with the last (Würm) glacial maximum.

SPATIAL AND TEMPORAL SAMPLING STRATEGY

The sampling rationale in time and space is keyed to two factors: (1) core coverage sufficient to define geographic ice-rafting patterns in the North Atlantic; and (2) stratigraphic control sufficient to delimit time intervals of significant climatic interest. I have chosen the long cycle of climatic change between deglacial terminations II (127,000 B.P.) and I (11,000 B.P.), because this interval has been recovered in numerous North Atlantic cores and is better defined stratigraphically than any other part of the late Quaternary record.

Geographically, the 32 cores (Fig. 1; Table 1) cover most of the subpolar North Atlantic, except shelves, shallow plateaus, abyssal plains, canyons, channels, and fans. Shelves and shallow plateaus rarely yield cores with planktonic microfossils needed for stratigraphic control and are overwhelmingly subject to re-erosion of sediments. Deep-ocean regions with highly reflective sediments were avoided, because input of coarse noncarbonate sand by turbidites masks ice-rafted input. Exclusion of these provinces still leaves coverage of two-thirds of the subpolar North Atlantic (Fig. 1).

Late Quaternary stratigraphic control in this ocean is excellent.[1] I have used four levels that were located, dated, defined, and discussed in earlier and ongoing studies (McIntyre and others, 1972; Ruddiman and Glover, 1972, 1975, and in prep.; Sancetta and others, 1973; Ruddiman and McIntyre, 1973, 1976): the zone 1 ash deposit at 9300 B.P.; the zone 2 ash deposit at 65,000 B.P.; and the warm faunal-lithologic equivalents of the Barbados I high sea level at 82,000 B.P. and of the Barbados III high sea level at 125,000 B.P.

The uppermost ash deposit (zone 1) is C^{14} dated at 9300 B.P. (Ruddiman and McIntyre, 1973). The two Barbados levels are part of an established dating framework developed for deep-sea sediments by many marine workers over the past 10 years. The salient parts of this dating scheme are summarized in Figure 2. The last two deglaciations were relatively abrupt; they were called "terminations" (I and II) by Broecker and van Donk (1970) and dated in Caribbean cores by $^{231}Pa/^{230}Th$ methods at 11,000 and 127,000 B.P., respectively (Broecker and Ku, 1969). Three prominent coral reefs indicative of high sea levels have been dated on Barbados at 82,000 B.P. (±4,000), 103,000 B.P. (±5,000), and 125,000 B.P. (±6,000) by Mesolella and others (1969). These abrupt cold-to-warm transitions and warm climatic peaks (high sea levels) provide a framework into which to tie North Atlantic climatic variations. [In addition to these correlations, unpublished data show the correlation of microfossil and lithologic variations with oxygen isotopic changes in four subpolar North Atlantic cores: V28-14 in the northwest; K708-7 in the northeast; and RE5-34 and V29-179 in the southeast (Fig. 1). The microfossil and lithologic changes forming part of the stratigraphy of this paper are thus matched to isotopic stages 1 through 5, which in turn have been

[1] A detailed listing of stratigraphic control levels is included in GSA supplementary material 78-1, which can be ordered from Documents Secretary, Geological Society of America, 3300 Penrose Place, Boulder, Colorado 80301.

Geological Society of America Bulletin, v. 88, p. 1813–1827, 8 figs., 4 tables, December 1977, Doc. no. 71213.

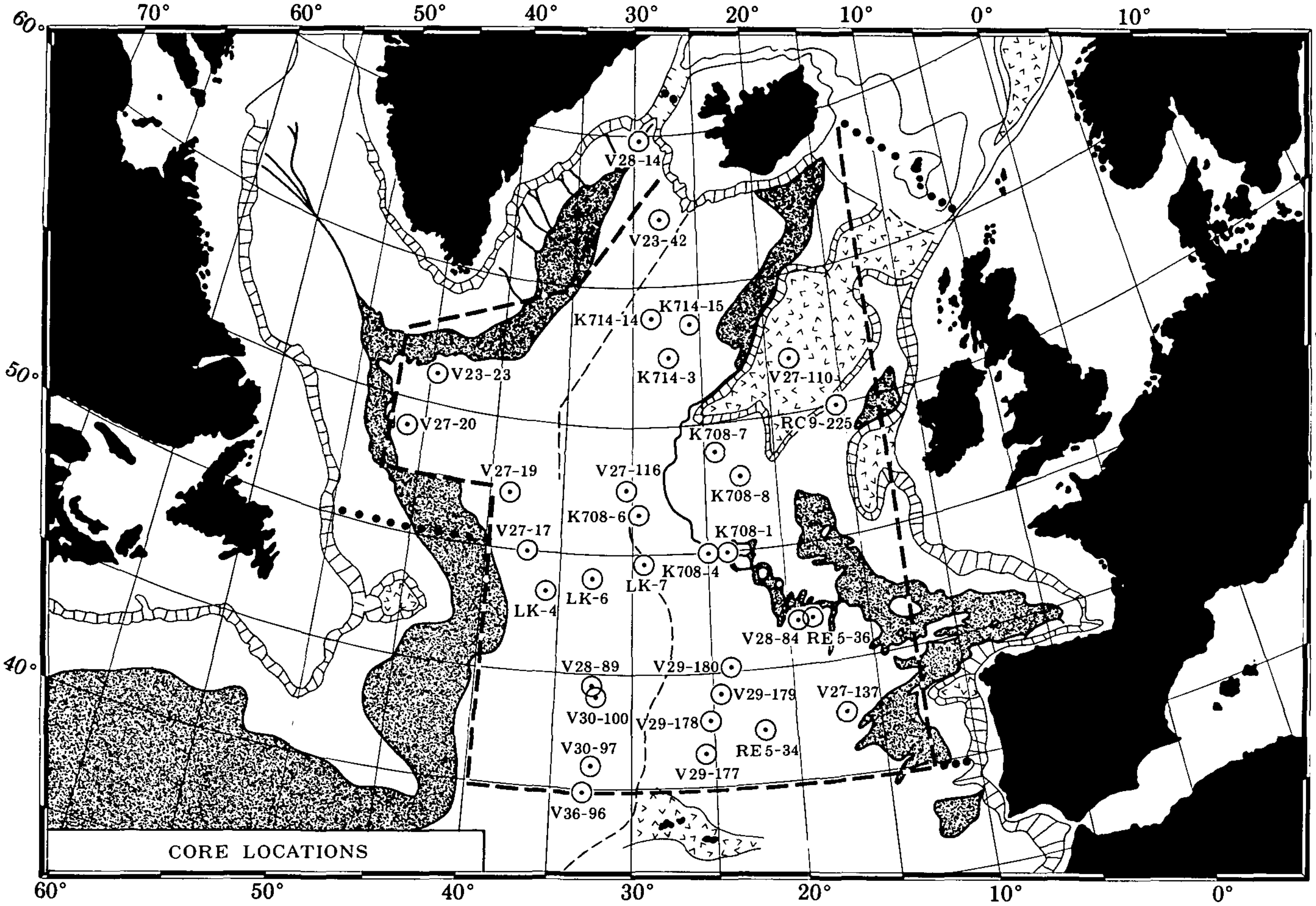

Figure 1. Locations of cores used in glacial detritus study (Table 1). Stippled pattern marks turbidite provinces: abyssal plains, fans, canyons, and channels. V pattern marks shallow offshore plateaus. Hachures delineate continental and insular slopes. Heavy dashed line encloses central subpolar area across which total ice-rafted input was integrated. Light dashed line shows mid-oceanic ridge crest. Dotted lines and continental slope (hachures) enclose additional peripheral region of ice-rafted input.

linked to the termination dating scheme (Broecker and Ku, 1969; Broecker and van Donk, 1970)].

To give some idea of how these stratigraphic components appear in North Atlantic data, a curve of estimated summer sea-surface temperature from core V23-82 (Sancetta and others, 1973) is plotted in Figure 2, along with the appropriate isotopic stage designations. The curve is plotted linearly to both core depth and time, with the core top taken as 0 yr and the next-to-last deglacial termination (II) at 795 cm as 127,000 B.P. From only these two depth with time alignments, warm temperature peaks appear at interpolated ages very close to the three Barbados high sea levels (Fig. 2).

This simple comparison can be repeated with a variety of faunal, floral, and lithologic curves in other subpolar North Atlantic cores (Fig. 1; Table 1). Most give comparably close correlations with the independent dating from Barbados. The warm levels in each core that appear correlative with the high stands of sea level at Barbados I (82,000 B.P.) and Barbados III (125,000 B.P.) were thus used as time with depth control levels for all feasible cores. Despite the time transgressiveness of deglacial warmings at these latitudes, the evidence indicates that these two peaks of sea-surface warmth are synchronous across the subpolar North Atlantic.

The age of the fourth control level (ash zone 2) was estimated at 65,000 B.P. by linear interpolation between terminations I and II in five cores (Ruddiman and Glover, 1972). More recent interpolations between the two terminations in 25 cores give an average estimated age for ash zone 2 of 64,700 B.P., with a standard deviation of ±3,500 yr on the interpolation (Ruddiman and Glover, in prep.).

There are also minor uncertainties involved in resolving the four control levels in this study. The synchronous ash-zone peaks are resolved to within an average of 2 cm for zone 1 (roughly 500 yr) and 1 cm for zone 2 (roughly 250 yr). The levels equivalent to Barbados I and III are defined by data at an average resolution of 5 cm (1,250 yr).

Each core was sampled between the control levels at depth intervals selected not to exceed average time increments of 3,300 yr. Between the zone 2 ash and Barbados I levels, this maximum interval was reduced to 2,500 yr and in most cores approached 1,000 yr. For all 32 cores in this study, a total of 1,448 samples was analyzed. All sample depths in the 32 cores were converted to time by interpolation between the four control levels, with several exceptions. Several cores lacked the zone 1 ash; for these I used as a control level the nearest time equivalent (faunal termination I), which ranges in age from 13,500 to 11,000 yr in different cores (see footnote 1). For cores lacking the zone 2 ash, I interpolated all ages between the Barbados I level and the upper control level (zone 1 ash or termination I). Three Lord Kelvin cores resurrected from Bramlette and Bradley (1941) did not reach the Barbados III level, and the Barbados I level has not yet been defined; only data between the two ash zones and slightly below the lower ash zone are included here for those cores.

"Glacial" and "interglacial" nomenclature is a problem for the last climatic cycle

TABLE 1. CORE LOCATIONS AND DEPTHS

Core	Lat (N)	Long (W)	Depth (m)
K708-1	50°00′	23°45′	4,053
K708-4	49°59′	25°01′	3,346
K708-6	51°34′	29°34′	2,469
K708-7	53°56′	24°05′	3,502
K708-8	52°45′	22°33′	4,009
K714-3	57°30′	27°32′	2,547
K714-14	58°57′	28°30′	2,143
K714-15	58°46′	25°57′	2,598
LK-4	48°29′	35°54′	3,955
LK-6	49°03′	32°45′	4,125
LK-7	49°32′	29°21′	3,250
RC9-225	54°59′	15°24′	2,334
RE5-34	42°23′	21°58′	3,750
RE5-36	46°55′	18°35′	4,500
V23-23	56°04′	44°33′	3,292
V23-42	62°11′	27°56′	1,514
V27-17	50°05′	37°18′	4,054
V27-19	52°06′	38°48′	3,466
V27-20	54°00′	46°12′	3,510
V27-110	56°54′	18°30′	1,264
V27-116	52°50′	30°20′	3,202
V27-137	42°42′	17°04′	4,883
V28-14	64°47′	29°34′	1,855
V28-84	46°55′	19°27′	4,206
V28-89	44°32′	32°35′	3,643
V29-177	41°32′	25°43′	3,391
V29-178	42°51′	25°09′	3,448
V29-179	44°01′	24°32′	3,331
V29-180	45°18′	23°52′	3,179
V30-96	39°57′	33°08′	3,188
V30-97	41°00′	32°56′	3,371
V30-100	44°06′	32°30′	3,519

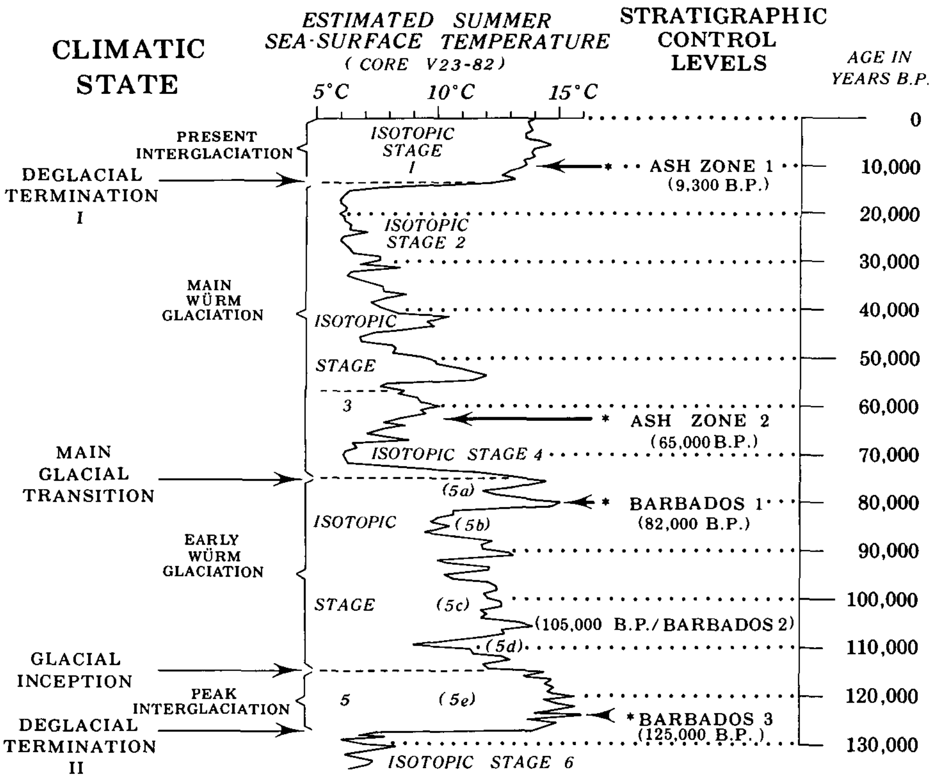

Figure 2. North Atlantic climatic curve based on estimated summer sea-surface temperatures in core V23-82 (from Sancetta and others, 1973). Levels used as control in other cores shown by asterisks and arrows on right. General Northern Hemisphere climatic conditions and prominent changes shown at left. Cores plotted to time by alignments noted in text. Placement of isotopic stages and terminations explained in text.

under study here. Most of the problem arises because local usages across the globe refer to widely varying intervals of time. The most direct evidence of ice-sheet growth — oxygen isotopic changes in the shells of benthic foraminfera — shows that initial Würm ice-sheet growth began in stage 5d at 115,000 B.P. (Shackleton and Opdyke, 1973). It is also clear from the same data that the major transition into the Würm glaciation occurred at 75,000 B.P. (the stage 5–stage 4 isotopic boundary). Both of these changes appear as prominent coolings in the North Atlantic record (Fig. 2). I have used in this paper the "glacial" or "interglacial" terminology shown on the left side of Figure 2; most periods of time are also referred either to isotopic stages or directly to years.

SAMPLE ANALYSIS

The samples were analyzed by the basic insoluble residue technique, except that the samples were first wet sieved through a 62-μm screen to isolate the sand fraction. Data in Molnia (1972) show that the > 500-μm fraction, which is the most unquestionably ice-rafted fraction, correlates well with the total > 62-μm fraction used here. The coarsest detritus is, however, more sporadic in occurrence. Consequently, gravel (>2 μm) was eliminated from the analyses.

Replicate tests of the modified insoluble residue technique indicated a mean analytical error of ±10.5%, with considerably lower errors (±4.7%) for samples rich in noncarbonate detritus. Much of the error was caused by moisture uptake in the filter paper. Because many analyses are combined into integrated averages, the precision error of the mapped values to follow is reduced to an estimated level of ±3%.

Cores V30-96, V30-97, V30-100, and V28-14 were analyzed by the procedure described in Kellogg (1975). (See footnote 1 to obtain a detailed description of analytical procedure and precision.)

DOWNCORE PERCENTAGE VARIATIONS OF NONCARBONATE SAND

In this section are presented downcore percentage data for coarse-fraction noncarbonate material in five cores representative of various sectors of the subpolar North Atlantic (Fig. 3). Because these data are converted to absolute input of coarse-fraction noncarbonate in the next section, I treat these percentage curves only as gross indices of time and space changes in ice-rafting input.

The southern, south-central, and central cores (Fig. 3) delimit a fundamental shift from low-percentage coarse-fraction noncarbonate material in cores to the south to higher percentages in cores from the central region. This limit is considerably sharper during main glacial climates and occurs at a latitude (43°N) that marks the southern limit of abundant ice-rafting (McIntyre and others, 1972; Ruddiman and McIntyre, 1976). Earlier studies lacked the regional coverage to fix this limit (Bramlette and Bradley, 1941)) or discussed the southern limits of ice-rafting primarily in terms of stray erratics found on seamounts far to the south (Pratt, 1961). Conolly and Ewing (1965) noted that noncarbonate detritus quantified as a percentage of the >74-μm fraction increased from negligible values south of lat 35°N to high values at lat 50°N. The lat 43°N limit correlates closely with the full-glacial polar-front position fixed from faunal and floral evidence by McIntyre and others (1972) and by CLIMAP (Climate/Long Range Mapping and Predictions; McIntyre and Kipp, with others, 1976).

Northwest core V27-20 (Fig. 3) shows a tendency for coarse-fraction noncarbonate percentage values in stage 5 to equal or even exceed the main glacial values. This suggests that ice-rafted deposition stays high during interglacial and early-glacial climates in the northwest. In fact, the modern axis of most abundant sea-ice and iceberg passage is located near this core (U.S. Naval Oceanographic Office, 1968). Moderate carbonate solution probably occurred in core V27-20, increasing the coarse-fraction noncarbonate percentages somewhat. Seasonal sea-ice cover during glacial climates may also have greatly reduced carbonate input.

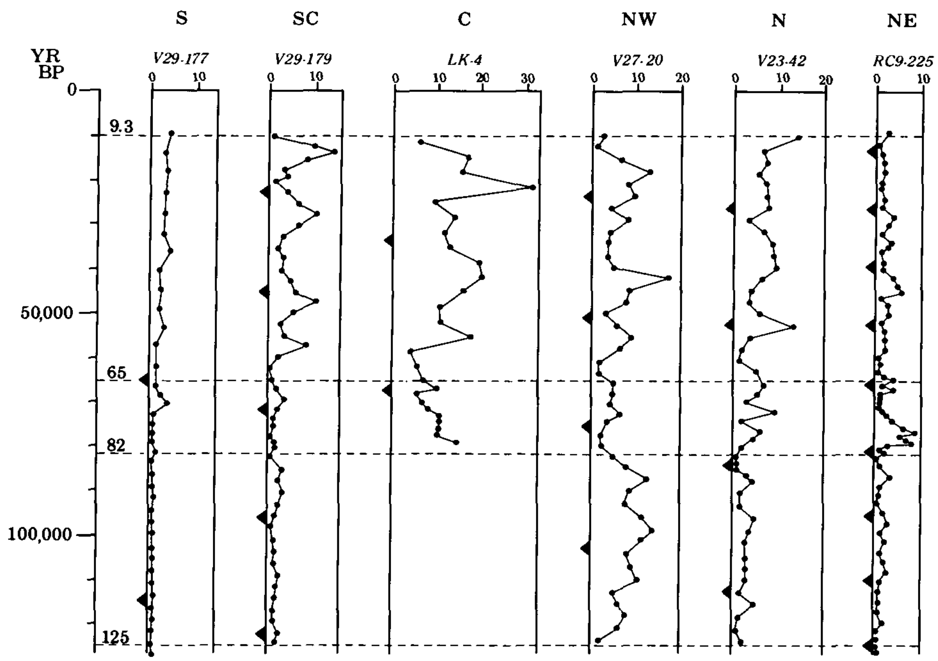

Figure 3. Downcore percentages of noncarbonate sand in five cores representative of major ice-rafting regions in North Atlantic. C = central; other letters are compass points. Cores plotted to time by alignment at four control levels: 125,000, 82,000, 65,000, and 9300 B.P. Depth in core in metres indicated by triangles down left side of core plots.

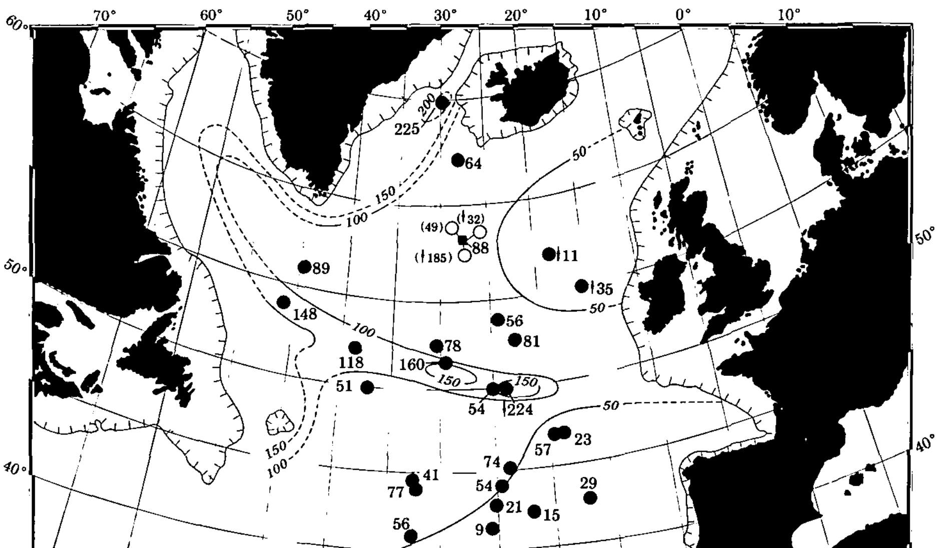

Figure 4A. Mean rate of deposition of ice-rafted sand in milligrams per square centimetre per 1,000 yr from 125,000 to 115,000 B.P. (isotopic substage 5e). Hachured line is continental shelf/slope break. This pattern (with Fig. 4B) is basic interglacial mode of deposition and largely resembles modern paths of sea ice and icebergs.

Northern core V23-42 and northeast core RC9-225 (Fig. 3) show a northward decrease in coarse-fraction noncarbonate percentages relative to cores in the central region (lat 50°N). Because of its location on the Feni drift, core RC9-225 has a sedimentation rate twice the regional norm due to bottom-current transport and to input of fine carbonate and noncarbonate, which diminish the already low coarse-fraction noncarbonate percentages by a factor of two. Cores K708-4 and K708-1 at 50°N, from Ruddiman and McIntyre (1976), have the highest coarse-fraction noncarbonate percentages in the study, thus suggesting an axis of maximum ice-rafting deposition in the central area.

Percentage data only suggest absolute ice-rafted input, because changes in other parameters may create artificial ice-rafting cycles. I have thus converted these percentage data to absolute input values.

ABSOLUTE INPUT OF NONCARBONATE SAND

Conversion of Percentage Data to Absolute Input

Calculation of absolute input rates of noncarbonate sand within specified intervals of core requires three steps: (1) determination of a mean sedimentation rate in centimetres per 1,000 yr for the specified interval; (2) multiplication by the mean bulk density of sediment in grams per cubic centimetre to obtain the total sediment input in milligrams per square centimetre per 1,000 yr; and (3) multiplication by the mean decimal fraction of noncarbonate sand (coarse-fraction noncarbonate) for all samples within the chosen interval of each core to obtain the input of ice-rafted sand in milligrams per square centimetre per 1,000 yr.

Step 1 is a direct by-product of the stratigraphic control (see footnote 1). Step 3 follows from the coarse-fraction noncarbonate percentage data analyzed (Fig. 3). In step 2, a sedimentation rate determined for lengths of core measured when the sediment was still wet is transformed into an equivalent input rate measured in grams of dry sediment. This is done because all later laboratory analyses are based on dry-sample weights.

Step 2 requires a bulk density expressed in terms of dry weight per wet volume. Dry weight/wet volume bulk density measurements have been made on four cores in this study by McIntyre and others (in prep.). These 20 measurements were made on lithologies varying from coccolith-foraminiferal oozes to glacial marine sediment. Despite substantial variations (as much as 20% around the mean), no clear correlation with sediment type emerged. The mean dry weight/wet volume bulk density of 20 measurements was just under 0.8 g/cm^3; I used this value for all step 2 conversions (Ku and others [1972] chose an identical bulk density as best representing a core from lat 42°N). This is an oversimplification, but systematic errors due to dry weight/wet volume bulk density variations around this mean value are not likely to exceed 20% over substantial lengths of core and are presumably much lower. Because the absolute input rates vary over a factor of 25 or 50, the errors from this oversimplification cannot dominate the mapped trends (Fig. 4).

Site-Factor Problems and Contouring Philosophy

Input rates of ice-rafted sand expressed in absolute units would seem to be the ultimate ideal, since absolute values are independent of changes in other components. There remains, however, a significant variation between nearby cores that cannot be assigned to any broad regional trends. I ascribe this variation (over a factor of 2 or 3) to "site-factor" redistribution of sediment, as discussed by Ruddiman and McIntyre (1976). Sedimentation rates can vary locally from core to core by a factor of 2 or 3, with all sediment fractions affected by the redistribution. Because all attempted methods used to normalize for this variability seem to inflict unjustified assumptions and greater noise on the data, I have chosen not to adjust the simple units of absolute input. Local (site-factor) noise remains obvious in the data.

The absolute input numbers on the maps here have been contoured in a literal manner, by linear interpolation of contours between actual core values, with four exceptions: (1) For three pairs of closely spaced cores (circles touching in Fig. 4), an average value was used. (2) For the three K714 cores centered on lat 58°N, long 28°W in a province of unusual sediment redistribution by bottom currents (Ruddiman and Bowles, 1976), I contoured on an average value at the geographic midpoint. (3) Around cores within sedimentation rates 50% higher or lower than the regional norm, I permitted a local smoothing of the contours if the input values violated the regional trends. These cores are marked on the maps in Figures 4A through 4G by arrows (indicating the need for correction to higher values because of low sedimentation rates, and conversely). (4) Finally, I contoured the exceptionally high input values in core V28-14 as a local phenomenon. This core lies in the axis of the Denmark Straits Channel and may have received "site factor" excesses of sediment by bottom currents or gradual downslope movements from the west, north, or east.

Choice of Map Intervals

Within the time limits of the stratigraphic coverage (125,000 to 9300 B.P.), I selected seven intervals for mapping the input of glacial sand (Table 2). The intervals cover periods ranging from 25,000 to 10,000 yr, and the mapped values for the various cores are based on an average of seven analytic determinations. Selecting shorter time intervals would have significantly increased core to core noise because of the lower number of samples averaged. The choices of these seven intervals were made on the basis of trends evident in the coarse-fraction noncarbonate plots in Figure 3, particularly near the central region of maximum percentages. I attempted to select intervals of significantly differing input rates; intervals

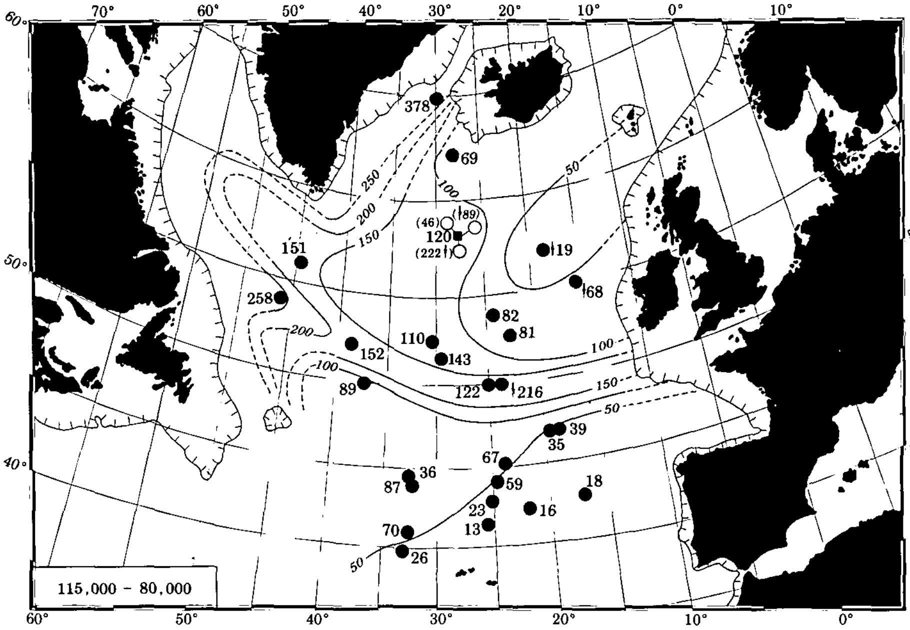

Figure 4B. Mean deposition rate from 115,000 to 80,000 B.P. (isotopic substages 5d to 5a). Slightly increased deposition evident from comparison with Figure 4A.

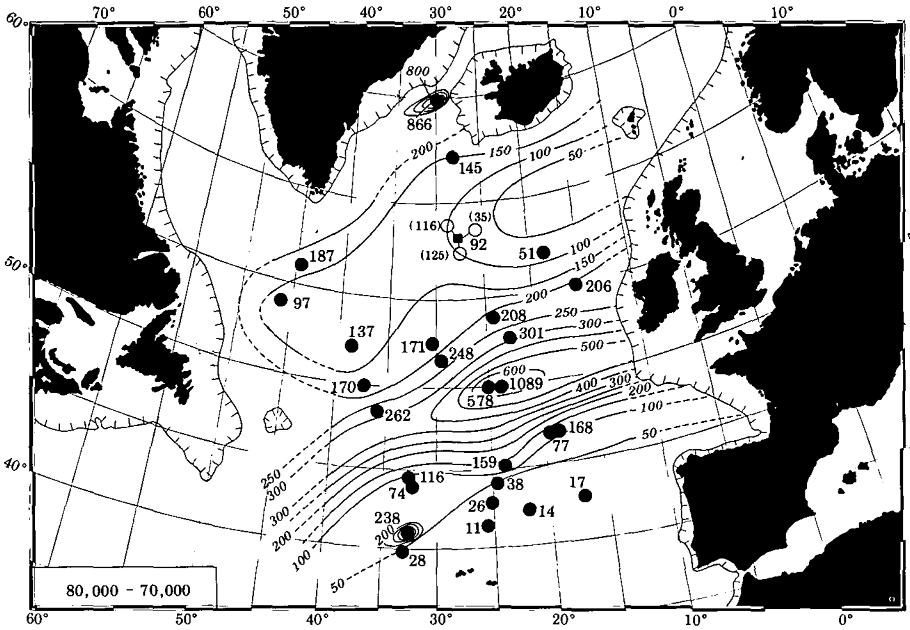

Figure 4C. Mean deposition rate from 80,000 to 70,000 B.P. (isotopic substage 4). This pattern (with Figs. 4D through 4G) is basic glacial mode of deposition. Major shift in depositional pattern and large increase in total abundance has occurred since intervals shown in Figures 4A and 4B.

1 and 2 were selected for low and low to moderate input, 4 and 6 for moderate input, 3 and 5 for high input, and 7 for very high input (Table 2; Fig. 3).

The early Würm glacial interval (2) was terminated early (at 80,000 B.P.) so as to not contaminate its relatively low coarse-fraction noncarbonate values with the higher values typical in the subsequent climatic cooling at 75,000 B.P. (Vertical mixing has no significant downward effect deeper than 5,000 yr in these cores [Ruddiman and Glover, 1972]). Interval 5 combines within one period two separate ice-rafting peaks marked in many cores at roughly 54,000 and 42,000 B.P. and separated by a period of slightly lesser input. Interval 7 was terminated at 13,000 B.P. because this is the earliest age of oceanic warming in this region (Ruddiman and McIntyre, 1973). The period 13,000 to 10,000 B.P. may have been more typically interglacial than glacial for the ocean near Great Britain.

Because of the large time interpolations between control levels at 65,000 and 9300 B.P. and those at 125,000 and 82,000 B.P., many of the ice-rafting curves show offsets of probably correlative percentage peaks, presumably due to interpolation errors. Most of these apparent age errors are a few thousand years; tests show that realigning the cores at these levels would not appreciably affect the mapped patterns and would raise judgment problems in many cores where the levels cannot be easily picked. Consequently, I have chosen to compute input values from straightforward linear age interpolations between the four control levels.

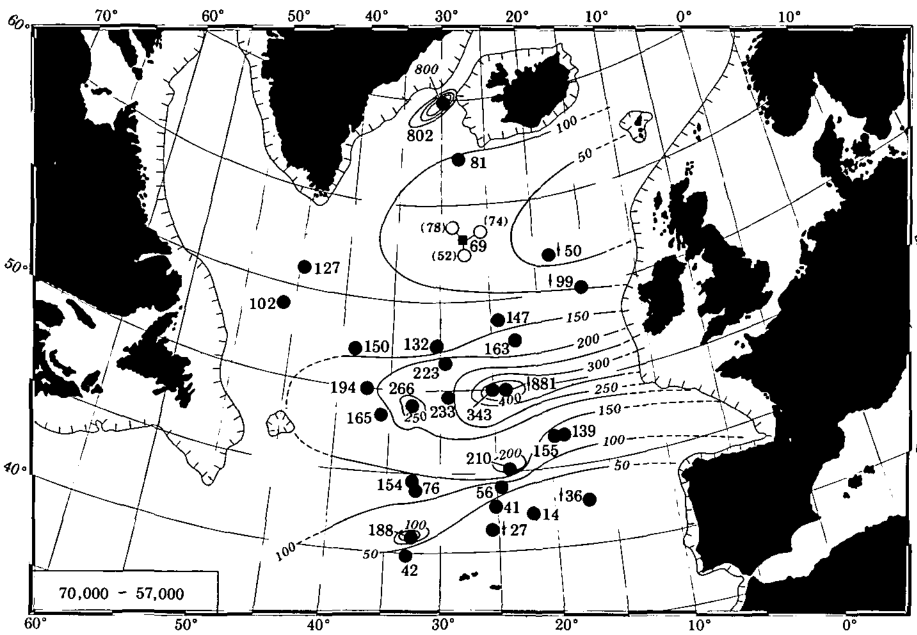

Figure 4D. Mean rate of deposition from 70,000 to 57,000 B.P. (lower part of isotopic stage 3).

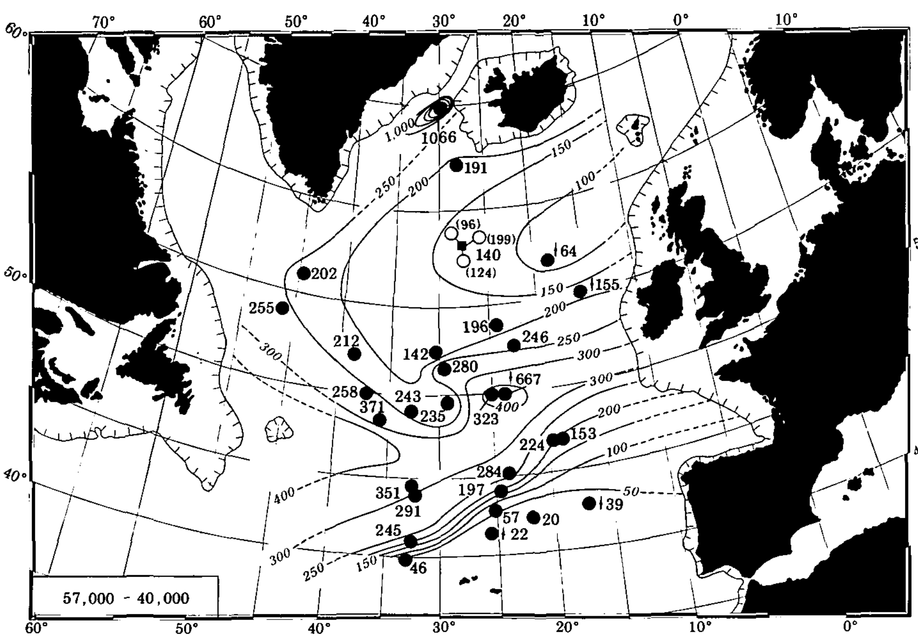

Figure 4E. Mean rate of deposition from 57,000 to 40,000 B.P. (middle of isotopic stage 3).

Maps of Absolute Coarse-fraction Noncarbonate Input

The geographic pattern of ice-rafted deposition from 125,000 to 13,000 B.P. takes two basic forms, beginning as a nearly longitudinal maximum in the northwest during interglacial (Fig. 4A) and early-glacial (Fig. 4B) climates and changing abruptly to an almost latitudinal maximum along lat 50°N during glacial climates (Figs. 4C through 4G). The midpoint of this fundamental shift in depositional mode occurs at about 75,000 B.P. and is bracketed between the 82,000 B.P. Barbados I level and the zone 2 ash at 65,000 B.P. The shift is due to strongly increased deposition along the lat 50°N axis. In the northwestern area of the interglacial and early-glacial depositional maximum, deposition rates during the main glaciation continue undiminished or even increase.

Several basic trends recur in all seven maps: a west- or west-southwest–trending region of high deposition between lat 43° and 53°N and centered on lat 47° to 51°N; an area of high deposition in the northwest along Greenland and Newfoundland; an area of very low to negligible deposition to the south of lat 40° to 43°N; and an area of moderately low to very low deposition to the northeast between Great Britain and Iceland. The discussion to follow will focus on variations in this basic pattern.

The interglacial pattern (125,000 to 115,000 B.P.) shows only a small secondary maximum along lat 50°N (Fig. 4A); in general, the sand rafted into the subpolar North Atlantic is deposited a short distance offshore of Greenland and Newfoundland. The early glacial pattern (115,000 to 80,000 B.P.) is similar, but deposition has increased slightly along a latitudinal axis at lat 50° to 53°N (Fig. 4B). Low values persist to the northeast and south of this secondary axis.

The first main Würm pattern (80,000 to 70,000 B.P.) registers a sudden shift, with deposition increasing roughly threefold across the eastern subpolar North Atlantic (Fig. 4C). The pattern takes on the basic glacial form along a maximum trending west-southwest at about lat 50°N. In this maximum, values are a factor of 5 to 10 higher than in the northeastern minimum. There is some evidence in this pattern for greatest deposition at the eastern end of the maximum. The second main Würm pattern (70,000 to 57,000 B.P.) registers lower values in the depositional maximum at lat

50°N and increased values in the southern and north-eastern minima (Fig. 4D). As a result, the input pattern is somewhat less concentrated along the lat 50°N maximum. Again, highest values occur in the eastern half.

In the next main Würm pattern (57,000 to 40,000 B.P.), a slight eastern maximum is still faintly suggested by the lobate twist of contours at lat 50°N, long 30°W (Fig. 4E). Deposition increases in the northeastern minimum, although values are still a factor of 5 lower than in the main axis. The fourth main Würm pattern (40,000 to 25,000 B.P.) is very similar to the one preceding; it differs primarily in the gradient defining the southern limit of major ice-rafting (Fig. 4F).

The last main Würm pattern (25,000 to 13,000 B.P.) shows the highest input of any interval in the eastern-central longitudes (Fig. 4G). This produces very strong north-south gradients around the lat 50°N maximum. Values in two cores just west of Ireland, however, were lower than at any level since the early Würm.

Norwegian Sea Input

Limited data are available from the Norwegian Sea on glacial sand input during the past 125,000 yr. Kellogg (1975) published downcore percentage variations for five Norwegian Sea cores, as well as one North Atlantic core included in this study (V28-14). Although precise stratigraphy in the Norwegian Sea has been much harder to obtain, I have taken Kellogg's three most prominent levels for control (termination II at ~127,000 B.P., termination I at ~11,000 B.P., and the glacial transition at ~75,000 B.P.). These were picked from faunal-lithologic data and may be subject to error of a few thousand years because of time transgressiveness. These three levels are the basis for calculating sedimentation rates during the interglacial and early-glacial (127,000 to 75,000 B.P.) and main-glacial (75,000 to 11,000 B.P.) intervals. As in the North Atlantic, a dry weight/wet volume bulk density of 0.8 g/cm^3 was assumed. Coarse-fraction noncarbonate mean percentage values during the two intervals were calculated from analyses in Kellogg (1975). Mean absolute input rates were then calculated as in the earlier section. The results (Fig. 5) suggest that the absolute coarse-fraction noncarbonate input values in the Norwegian Sea vary only slightly from glacial to interglacial climates. On the average, main-glacial values are slightly higher, but stratigraphic uncertainties eliminate any significant difference. Both maps show a significant increase in absolute input toward Norway to the southeast, where Holtedahl (1959) showed high percentage values of coarse-fraction noncarbonate during the late Würm. The high main-glacial value in northernmost core

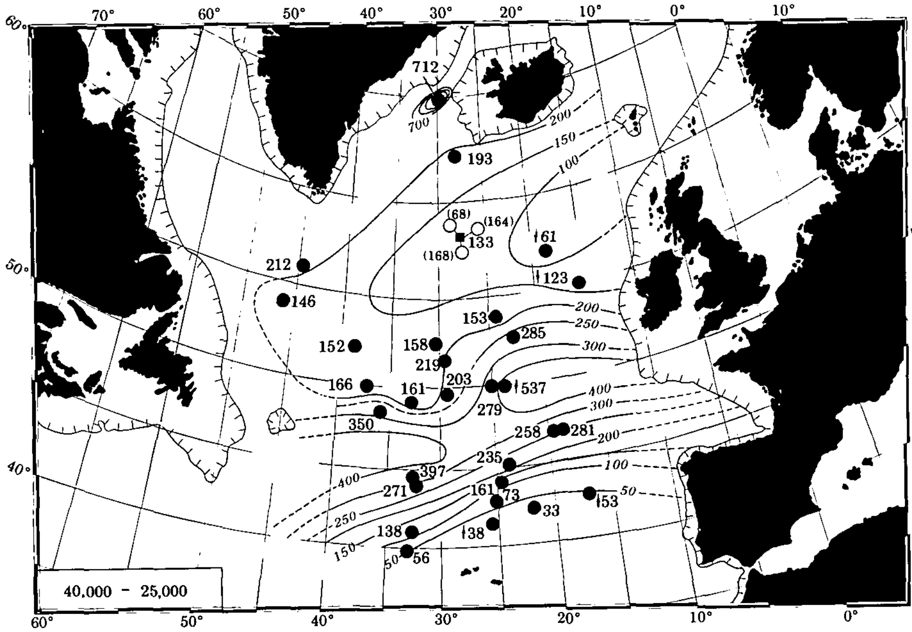

Figure 4F. Mean rate of deposition from 40,000 to 25,000 B.P. (upper part of isotopic stage 3).

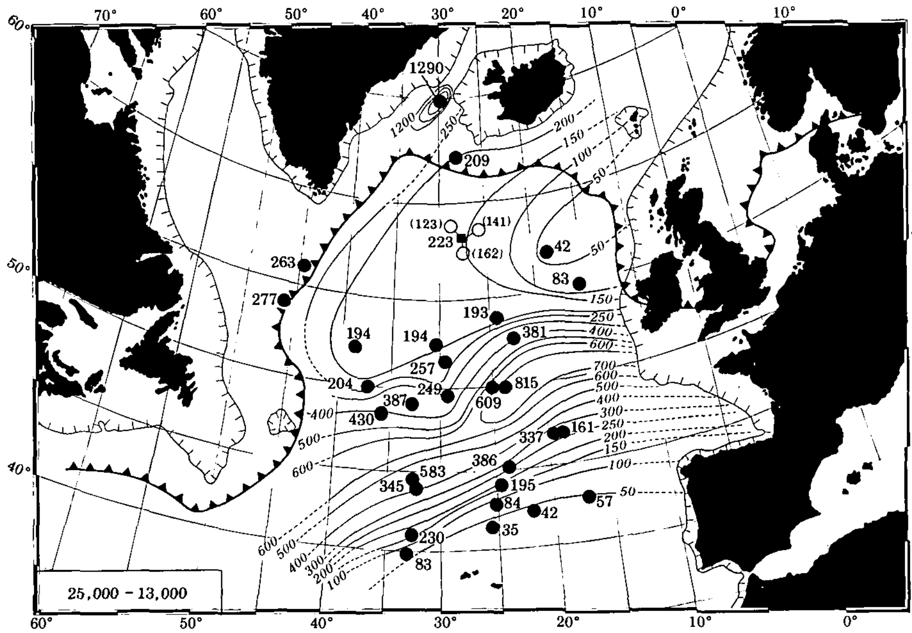

Figure 4G. Mean rate of deposition from 25,000 to 13,000 B.P. (isotopic stage 2). Line with triangles is ice-sheet limit on continents and inferred ice limit over ocean (Hughes and others, 1977).

TABLE 2. INTERVALS MAPPED FOR ABSOLUTE GLACIAL DETRITUS INPUT

Interval	Equivalent isotopic stages*	Time spanned (yr. B.P.)†	No. of cores mapped	No. of samples per core for each interval: Range	Avg
1. Peak interglacial	5e	125,000 to 115,000	29	4–12	7.8
2. Early Würm	5d to 5 a	115,000 to 80,000	29	6–21	10.3
3. Main Würm	4	80,000 to 70,000	31	3–13	5.4
4. Main Würm	3 (lower)	70,000 to 57,000	32	3–10	5.5
5. Main Würm	3 (middle)	57,000 to 40,000	32	4–11	6.9
6. Main Würm	3 (upper)	40,000 to 25,000	32	4–10	6.2
7. Main Würm	2	25,000 to 13,000	32	3–7	4.7

* From Emiliani (1955, 1966) and Shackleton (1969).
† See section on stratigraphy for time control and related assumptions.

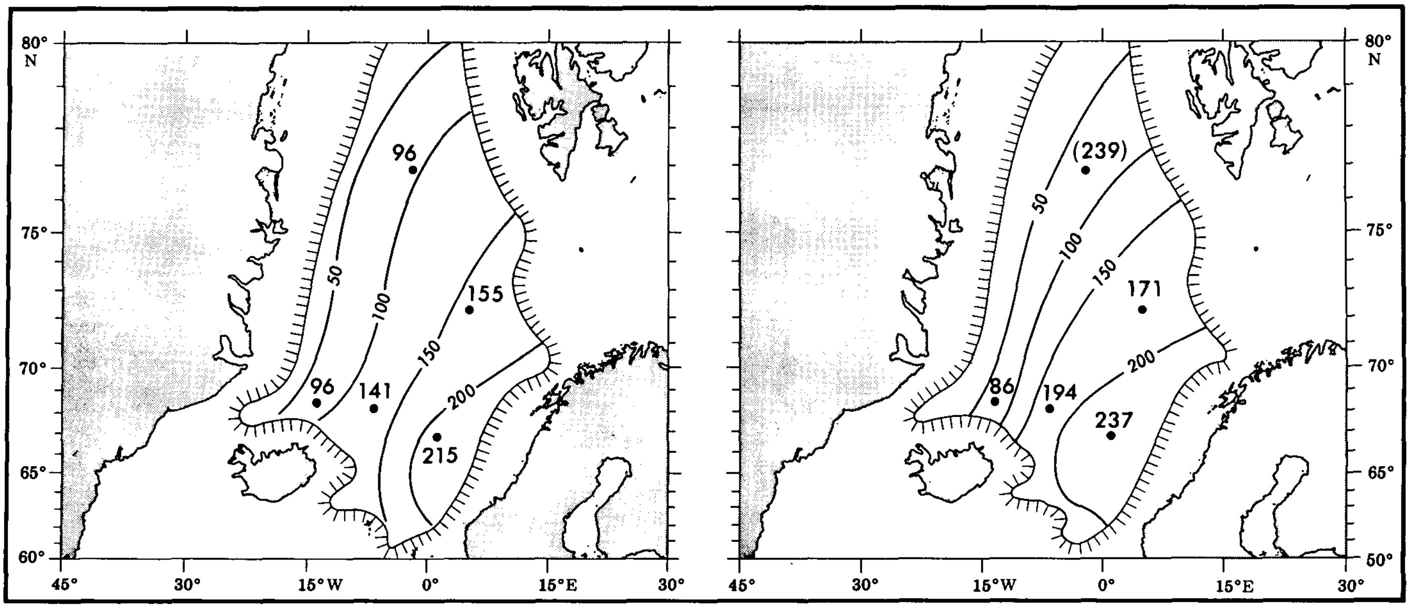

Figure 5. Left: Mean interglacial and early-glacial rate of input of ice-rafted sand, in milligrams per square centimetre per 1,000 yr from 127,000 to 75,000 B.P. in Norwegian Sea. Calculations based on data in Kellogg (1975). Hachured line delineates shelf break or slightly deeper areas thought to have been situated beneath grounded ice sheets during glacial conditions. Right: Mean main-glacial input rate from 75,000 to 10,000 B.P. in Norwegian Sea. Pattern is very similar to interglacial and early-glacial deposition (left).

V28-25 (Fig. 5) breaks this otherwise steady trend; I arbitrarily chose to regard this value as being of only local (site-factor) significance and ignored it in the regional contouring.

ICE-RAFTING AND PALEOCIRCULATION

Few means are available for reconstructing actual trajectories of past oceanic circulation. Microfaunal and microfloral estimates of paleotemperature, paleosalinity, and paleodensity (σ_T) by any of several methods (Imbrie and Kipp, 1971; Hecht, 1973) can ideally be used to infer the mean direction of the pure gradient current at, or slightly below, the sea surface. Berger and Gardner (1975), however, offered reasons for suspecting salinity estimates, even though the dominant ecological parameter (temperature) may be accurately reconstructed. With this uncertainty, estimates of paleodensity (and hence reconstructions of the mean gradient current) are also suspect.

Ice-rafted detritus provides a supplementary approach to reconstructing paleocirculation, since the melting ice leaves behind a permanent carpet of detritus that in some manner marks its trajectory across the ocean. Usually, the depositional patterns reveal more about the primary melting locus of sediment-laden ice (Watkins and others, 1974) than about the trajectories of ice passage. Combined with microfaunal reconstructions of water mass movements and paleotemperature changes, the patterns of ice-rafted deposition may yield valuable information on both melting and delivery.

Changes in the Polar Water Mass

As shifts occurred in the axis of deposition of ice-rafted detritus, the polar water mass,[2] defined by dominance of the polar foraminifer *Globigerina pachyderma* (s.), also migrated across subpolar latitudes (McIntyre and others, 1972; Ruddiman and McIntyre, 1973). The abundance of *G. pachyderma* (s.) during the past 125,000 yr in representative cores across the subpolar North Atlantic is shown in Figure 6. Percentages greater than 60% indicate the presence of polar water. The faunal-count depths are interpolated to age by alignment at the same control levels used for the ice-rafted detritus (see footnote 1). The cores portray conditions across lat 50° to 55°N, from the comparatively frigid western Atlantic to the warmer eastern sectors (core locations in Fig. 1 and Table 1).

The faunal data in Figure 6 show two intervals of particularly significant polar-water advances during the last interglacial-glacial cycle. During the first such advance at about 115,000 B.P., polar water expanded to fill the Labrador Sea and areas just east of Greenland and Newfoundland. The only subsequent retreat of polar water from this region prior to the recent deglacial polar front retreat at 9000 B.P. was a brief warming at about 82,000 B.P. (Fig. 6).

[2] This "water mass" is an ecological phenomenon because it is defined by faunal data. It appears usually to have been bounded along its equatorward limit by a polar frontal system with considerable temperature-salinity expression.

The central North Atlantic cores (V27-19, V27-17) show short-lived eastward advances of polar water just after 115,000 B.P. and at roughly 95,000 B.P. The largest change in this region, however, was the second major advance of North Atlantic polar water at 75,000 B.P. Except for very brief intervals, central subpolar waters did not again warm sufficiently to break the polar faunal dominance until the polar-front retreat at 11,000 B.P.

The northeastern cores (K708-8, K708-1, RC9-225) show much lower polar-faunal percentages than the north-central cores throughout the period 127,000 to 75,000 B.P. Only with the strong polar-water advance at 75,000 B.P. did the polar fauna first dominate in this region. Subpolar species temporarily broke the polar faunal dominance several times during the main glacial interval (particularly in core RC9-225 close to Great Britain) before the polar front retreat at 13,500 B.P.

Cores south of lat 43°N do not record polar-faunal percentages high enough to indicate the presence of polar water at any time in the last interglacial-glacial cycle (McIntyre and others, 1972). This is also the southernmost limit of polar water at 18,000 B.P. along the polar front reconstructed by CLIMAP (McIntyre and CLIMAP project members, 1976).

In summary, waters overlying cores to the west and northwest were uniformly colder during the last 125,000 yr than those over cores to the east and south, as they are today. This pattern suggests a net cyclonic flow in the subpolar gyre as at present, with southward Arctic outflow a constant fea-

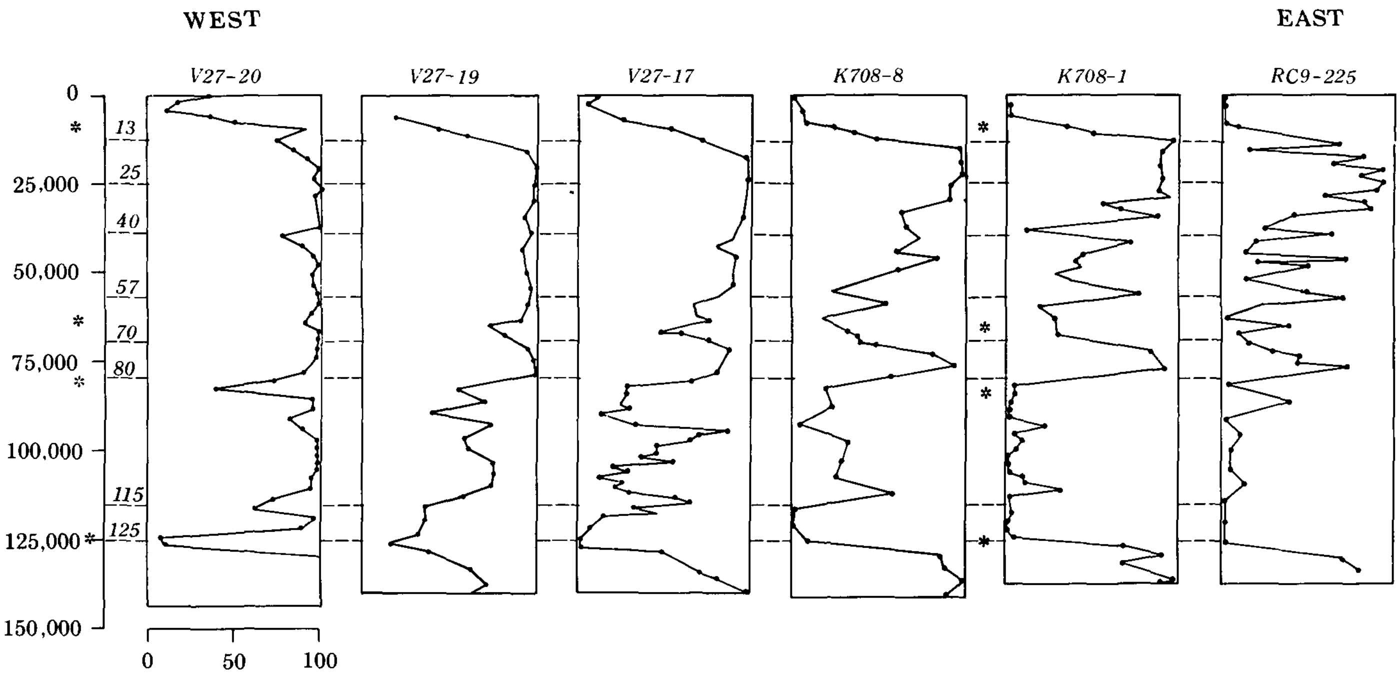

Figure 6. West-east transect across subpolar North Atlantic at lat 50° to 55°N. Plot shows abundance of *Globigerina pachyderma* (s.) as percentage of total planktonic foraminiferal population. Cores plotted to time between same control levels (marked by asterisk) used to plot noncarbonate sand (Fig. 3). Ice-rafting intervals mapped in Figures 4A through 4G marked by dashes. Faunal evidence shows that waters to east near Great Britain stayed warmer than those to west in Labrador Sea near Greenland during all climates.

ture in the west and advection of more temperate water northward equally typical in the east. The faunal data show that the most significant eastward advances in mean position of the polar front occurred at 115,000 B.P. and 75,000 B.P.

Absolute Input Maps and Paleodelivery Pattern

Delivery and deposition of ice-rafted detritus in the North Atlantic Ocean occur in two basic modes, one glacial and one interglacial. The interglacial depositional mode (Fig. 7A) largely resembles the form of modern iceberg and sea-ice occurrence (U.S. Naval Oceanographic Office, 1968). The three northwesternmost cores in this study (V23-23, V27-20, and V28-14) lie just along the observed maximum seaward extent of abundant ice during the past 75 yr. Since last interglacial (as well as early-glacial)deposition was highest in these same cores (Figs. 4A, 4B), no great departure from the modern circulation pattern is demanded.

In the last interglacial Atlantic pattern, polar ice flowing out from the Norwegian and Labrador Seas met warmer North Atlantic Drift water, melted, and dropped detritus along the coasts of Greenland and Newfoundland (Figs. 4A, 7A). This interglacial mode was (and is at present) a weak net cyclonic gyre, with northward-flowing North Atlantic Drift water dominating much of the subpolar latitudes. Polar ice and water were for the most part restricted to a small northwestern part of the Atlantic.

There is one element in the interglacial pattern that is not explained by the present circulation. The axis of increased deposition along lat 51°N during the last interglaciation (Fig. 4A) suggests a statistical preference for iceberg penetration eastward along that latitude. No such tendency emerges from the admittedly sparse iceberg data, which show sporadic sitings in a fairly random pattern over the central and eastern North Atlantic (U.S. Naval Oceanographic Office, 1968).

The early glacial depositional pattern (Fig. 4B) is very similar to the peak interglacial pattern (Fig. 4A), with a minor increase in ice-rafted input. In fact, the early-glacial pattern belongs to the interglacial type (Fig. 7A). However, the prominent cooling at 115,000 B.P. in the Norwegian and Labrador Seas may have brought early-glacial increases in ice-rafting that could not be detected because of geographic or stratigraphic deficiencies in this study.

The main glacial pattern of ice-rafted deposition (Fig. 7B) was very different. Its basic form was established during the abrupt climatic change at 75,000 B.P. and underwent only minor variations during subsequent intervals. It differs from the interglacial pattern primarily in reflecting the passage of ice farther from the pole before reaching water warm enough in which to melt. The oceanic circulation responsible for ice delivery to the primary melting zone remained what it had been during the interglaciation and early glaciation: a basically cyclonic regime.

The juxtaposition of a northeastern depositional minimum just off Great Britain against higher values to the northwest near Iceland and Greenland reveals the basic sense of ice delivery. The faunal data (Fig. 6) show that waters northwest of Great Britain (for example, core RC9-225) were invariably warmer than those just east of Greenland and Newfoundland (for example, core V27-20). This potential to melt any passing ice means that the northeastern depositional minimum was also a significant ice-passage minimum relative to the northwestern sector. To avoid passing through and melting in this depositional minimum, most Scandinavian ice entering the North Atlantic must have moved in a large counterclockwise loop, first passing westward toward Iceland, then southwestward and southward upon entering the subpolar North Atlantic (Fig. 7B). Glacial depositional values in the northwestern Atlantic off Greenland are comparable to or higher than the interglacial levels despite much colder waters that should inhibit melting; this suggests much greater ice passage southward along that axis.

I infer that Laurentide and Greenland glacial ice entering the western subpolar North Atlantic in the Labrador Sea traveled southeast, joined the ice outflow from the Norwegian Sea, and melted along the band of maximum ice-rafted deposition at lat

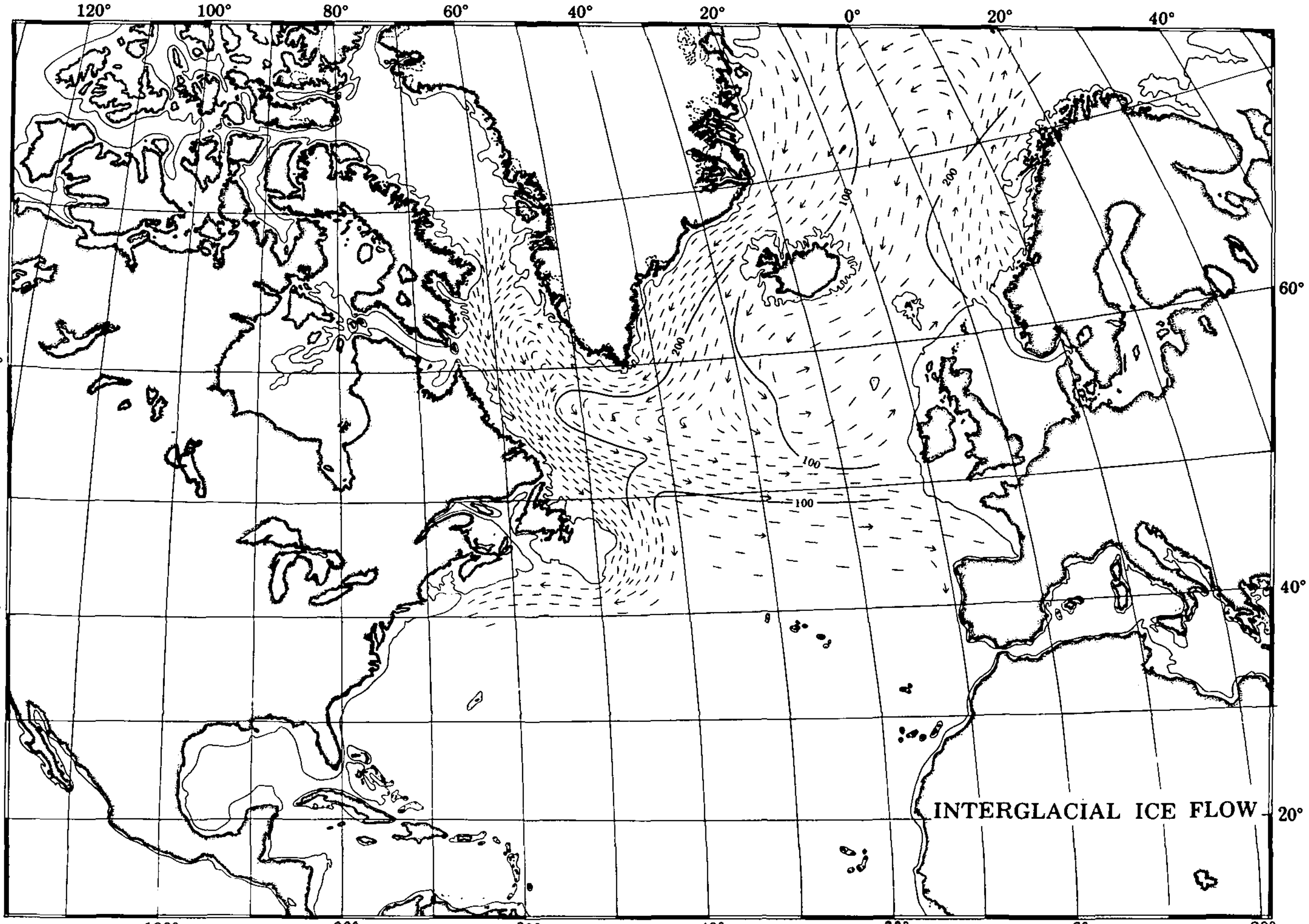

Figure 7A. Inferred mean paths of delivery of ice-rafted detritus during an interglacial regime. Sizes of continental ice masses are variable and not shown. Main distribution pattern (dashes) largely follows present-day flow of sea ice and icebergs, except for secondary flow axis to east-southeast across lat 51°N. Mean depositional rates of ice-rafted sand (in milligrams per square centimetre per 1,000 yr) cover last interglacial and early-glacial period from 125,000 to 80,000 B.P.

50°N (Fig. 7B). This high-deposition zone must have marked a strong convergence between cold, ice-laden polar waters moving to the southeast and warmer North Atlantic waters flowing to the northeast.

I assume that westerly winds prevailed over the band of maximum deposition. Even at the intense late Würm glacial maximum, wind-blown redistribution of outwash loess (Flint, 1971) indicates that westerly winds dominated at least as far north as the ice-sheet margins (lat 40°N in eastern North America, and 50°N in Europe). During most of main-glacial time, the less severe climate and smaller ice extent point to a more constricted region of polar easterlies and northerlies. Westerly to southwesterly winds should then have prevailed across the main band of ice-rafted deposition, driving ocean currents and ice from west to east in the West Wind Drift.

The glacial pattern (Fig. 7B) does not rule out direct ice-rafting of sand from the western part of the ice sheet on northern Great Britain into the easternmost part of the high-deposition axis. Input close to the northwest coast of Great Britain is indeed reasonable, but little deposition farther seaward of this small source area was likely in the prevailing West Wind Drift.

The English Channel was largely emergent during the main-glacial period, barring westward flow into the Atlantic of ice from glacial lakes south of the Scandinavian ice sheet. Some of the Scandinavian ice flowed in ice streams out through the Norwegian Channel and turned north in the Atlantic along the coast of Norway (Fig. 7B). Holtedahl (1955) found that a significant minor component of the detritus on the Norwegian continental terrace at lat 62° to 64°N had been ice-rafted northward from distinctive larvikite and rhomb-porphyry sources in the Oslo-Skagerrak area of the Baltic Sea. Large quantities of western Scandinavian ice flowed directly into the easternmost Atlantic and turned north in the prevailing oceanic flow.

Interpretation of glacial circulation in the Norwegian Sea and Labrador Sea is complicated by uncertainties about the distribution and thickness of marine ice. Kellogg (1975) deduced a permanent sea-ice cover on the entire Norwegian Sea for the main Würm glaciation (75,000 to 11,000 B.P.). Hughes and others (1977) have theorized that the Norwegian and Labrador Seas were covered by a marine ice sheet several hundred metres thick by late Würm time, but they did not infer when the ice thickened. On the other hand, Flint (1971) supposed that there was open water in the southeastern Norwegian Sea even at the late Würm glacial maximum. Recent coccolith evidence (A. McIntyre, 1976, personal commun.) suggested that the southeastern Norwegian Sea remained ice-free throughout the last interglaciation and most of the early glaciation, and during minor parts of the main glaciation.

These various theories impose different limits on the circulation responsible for the high-latitude ice-rafting patterns. For example, the weak depositional maximum in the southeastern Norwegian Sea could

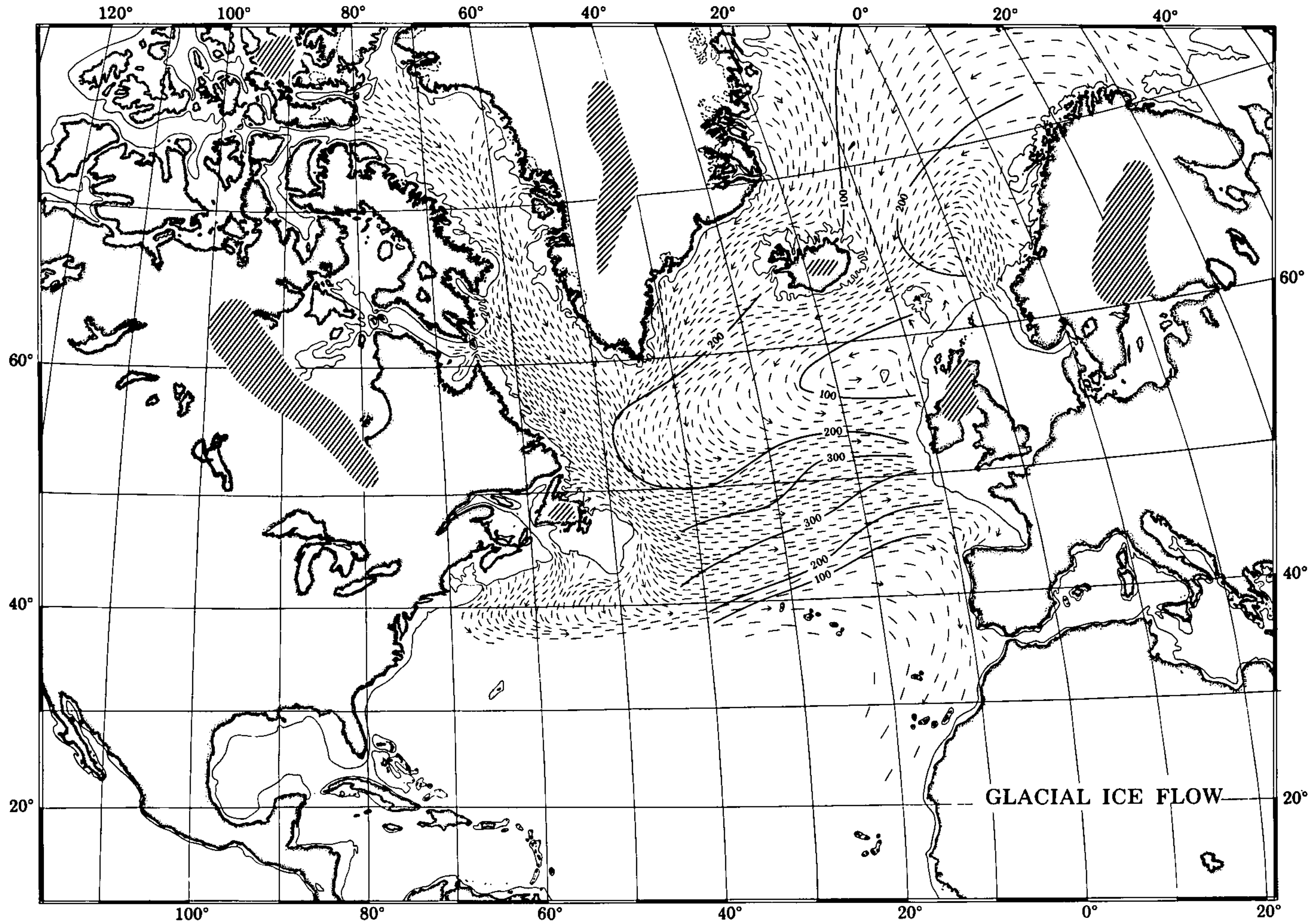

Figure 7B. Inferred mean paths of distribution of ice-rafted detritus during a main glacial regime. Diagonal-ruled areas = spreading centers of continental ice sheets. Oceanic distribution pattern (dashed lines) is basically cyclonic as during interglacial regime and at present.

mark either (1) melting of northward-moving icebergs and deposition in open water, (2) melting from the bed load of Scandinavian icebergs incorporated into slowly drifting Arctic pack ice after calving from the Norwegian coast, or (3) bed-load deposition beneath fast, southward-moving ice streams in a marine ice sheet connected back upflow to the Scandinavian and Barents continental ice sheets. These completely different explanations could account for the same pattern during different climatic periods. Analogous uncertainties exist in the Labrador Sea area, which may have seen increased ice cover at and after 115,000 and 75,000 B.P.

There is too much uncertainty at present to prove one alternative. I infer that the secondary glacial depositional maximum in the cold and largely ice-covered southeastern Norwegian Sea primarily reflects dropping of bed-load detritus from Scandinavian ice as it first enters the ocean. Not much melting need have occurred to create this maximum, which is probably indicative primarily of nearness to source.

It is likely that most of the British and Scandinavian ice carried northward into the Norwegian Sea eventually turned to the west and southwest under the influence of polar easterlies and northerlies (Fig. 7B). From the depositional patterns shown in Figure 4, it seems likely that the European ice then joined Arctic ice (presumably including significant amounts of sediment-bearing berg ice from the Barents ice shelf) and flowed to the south or southwest out of the Norwegian Sea (Fig. 7B). Although passage into the subpolar North Atlantic Ocean could have occurred on either side of Iceland, the more prevalent glacial ice cover in the Denmark Straits made an easterly passage more likely than it had been during interglacial and early glacial flow. The northeastern depositional minimum suggests that the flow then turned abruptly westward south of Iceland. Higher deposition along Greenland probably reflects still more dropping of bed load during passage south.

After transiting south of lat 55°N, the European-Arctic ice outflow then turned to the east in the prevailing westerly winds, entered the high-deposition band at lat 50°N from the north or northwest (Fig. 7B), melted, and dropped most of its load. Presumably, relatively few icebergs survived the subsequent west-to-east passage along lat 50°N in the rough waters near the main-glacial polar front. The depositional minimum to the northeast does not allow the major iceberg flow to have turned north along the coast of Great Britain. Kudrass (1973) found high late-glacial depositional rates of noncalcareous sand on the Portugese continental slope. Although this detritus may have been in part emplaced by downslope and across-slope currents, it may also be evidence that much of the surviving ice turned south in a very narrow band along the coast of Portugal. In any event, the great majority of European detritus ice-rafted into the central subpolar North Atlantic arrived circuitously in a vast cyclonic loop and not directly by an east-to-west path.

The ice-rafting depositional axis trending west-southwest along lat 46° to 50°N may mark the mean glacial location of warm subpolar water along the southern limit of the polar front or convergence. This position lies about 5° north of, but exactly parallel to, the extreme full-glacial polar-front position defined from biotic evidence by CLIMAP (McIntyre and CLIMAP project members, 1976). The depositional axis shows no significant shifts during any of the five main glacial subintervals (Figs. 4C through 4G), suggesting a surprising long-term stability of the glacial polar convergence.

In short, there are two depositional modes of ice-rafted detritus: interglacial (Fig. 7A) and glacial (Fig. 7B). These result from very similar delivery paths of ice-rafted detritus; the differences mainly reflect change in the locus of melting and not in the circulation responsible for ice delivery.

FLUCTUATING ICE-RAFTED INPUT DURING LAST GLACIAL-INTERGLACIAL CYCLE

I have used the contours in Figure 4A through 4G to calculate the mean input rate of ice-rafted sand per millenium across the central subpolar North Atlantic during each of the seven subdivisions of the last interglacial-glacial cycle (Table 3). The inputs were determined for the area shown by the heavy dashed line in Figure 1. To extend the calculations outside the main study area, I relied on the less rigorous contours shown by dotted lines in Figures 4A through 4G and on the contours in the Norwegian Sea (Fig. 5). This additional input of sand in the subpolar Atlantic north of lat 40°N and in the Norwegian Sea is plotted with dashed and dotted lines in Figure 8 and listed in Table 4. A small but potentially important area near Flemish Cap is excluded from these calculations because of no core coverage. All continental shelf and shallow plateau areas are excluded from the calculations for reasons stated previously.

These data show a particularly abrupt increase in rates of ice-rafted input at 75,000 B.P. superimposed upon a generally growing input from low values early in the last interglaciation (125,000 to 115,000 B.P.) to maximum values in the late Würm glaciation (25,000 to 13,000 B.P.). Changes in both patterns and input rates thus suggest that the main ice-rafting transition occurred at 75,000 B.P. This transition lags by some 40,000 yr the glacial inception at 115,000 B.P. (Fig. 2).

Data from Shackleton and Opdyke (1973) show the lowering of relative sea level inferred from oxygen isotope data primarily reflecting ice storage on land (Fig. 8). They attribute most of the variation in the isotopic ratios to changes in size of Northern Hemisphere glaciers. The comparability of these two plots is significant: each increment of additional ice stored on land leads to a roughly proportional increment of additional detritus rafted to the deep ocean. This link puts some limit on where the ice accumulates during the early stages of glaciation, although the problem could be very complex. Warncke (1970) cautioned against using ice-rafted debris (in the Antarctic) as an indication of climate and ice-sheet size. To his many arguments can be added other complexities peculiar to Northern Hemisphere ice: the problem of multiple ice centers not necessarily growing and shrinking exactly in phase; the debate as to whether ice sheets first nucleated as coastal mountain glaciers (Flint, 1943) or as perennial snow fields on upland plateaus (Ives and others, 1975); and many uncertainties as to the basic structure, geographic extent, bed conditions, and flow patterns of Northern Hemisphere ice during different stages of the Würm glaciation. Despite these uncertainties, it is clear that the early ice sheets must have nucleated in regions where they could feed icebergs to the ocean with little or no delay. They could have formed either in coastal mountains, with icebergs calving directly from marine termini, or in areas farther inland, with passage to the ocean by way of ice streams through inland seas. In either case, no large lag (more than a few thousand years) between ice sheet formation and ice-rafted delivery and deposition is possible.

TOTAL VOLUME OF ICE-RAFTED INPUT

The total ice-rafted input of the sand fraction across the area shown in Figure 1 from 125,000 to 13,000 B.P. is 1.4×10^{18} g. Total input of all detritus (including lutite) for these intervals can be estimated by using data on fine-fraction abundance from Ruddiman and McIntyre (1976), who concluded that the noncalcareous lutite in several cores was a constant factor of about 6 more abundant by weight than the noncalcareous sand (6.3 in main-glacial climates, 6.0 in interglacial and early-glacial times). The constancy of this ratio, as well as the selection of cores from provinces of little regional bottom-current transport and eolian influx, pointed to a probable ice-rafted origin for the noncalcareous lutite (as well as sand). This ratio was thus used to calculate a total ice-rafted input of 9.8×10^{18} g during the period 125,000 to 13,000 B.P. This calculation omits the region just east of Flemish Cap, as well as the region off the North American coast south and west of the Grand Banks (Fig. 1). Inclusion of this area could add considerably to the total. On the other hand, it is likely that some of the lutite input in the western North Atlantic near Greenland and Labrador was not ice-rafted but wind-blown or storm-suspended. This would reduce the estimates.

The long record of core K708-7 (Ruddiman and McIntyre, 1976) shows rates of ice-rafted input in the North Atlantic through the past 600,000 yr that are similar to the past 125,000 yr. Evidence from North Pacific ice-rafting (Kent and others, 1971) and from isotopic data (Shackleton and Opdyke, 1973) suggests analogous Northern Hemisphere variations in glacier size and ice-rafting since 1.2 m.y. I thus estimate by simple linear extrapolation that the total volume of ice-rafted deposition in the North Atlantic since 1.2 m.y. has been an order of magnitude higher than that between 125,000 and 13,000 B.P.: 15×10^{18} g of sand and 100×10^{18} g of all noncalcareous detritus. A linear extrapolation is warranted since earlier cycles were similarly apportioned between cold and warm climates. For the full 3 m.y. of Northern Hemisphere ice-rafting (Berggren, 1972), I estimate a total ice-rafted mass of at least 150×10^{18} g in the subpolar North Atlantic.

There is little sense in trying to calculate mean erosion depths for the Laurentide, Greenland, Barents, and Scandinavian ice sheets during Pleistocene time, because of extreme local variability on land (Flint, 1971). It is possible, however, to reverse this procedure and determine from the preceding calculations how thick a layer could be spread across the glaciated parts of the continents and shelves by excavating all ice-rafted detritus from the North Atlantic and Norwegian Sea.

TABLE 3. AVERAGE INPUT OF GLACIAL MARINE SAND DURING SEVEN SUBINTERVALS OF LAST INTERGLACIAL-GLACIAL CYCLE

Interval (yr B.P.)	Central subpolar Atlantic	Peripheral subpolar Atlantic	Norwegian Sea	Total
125,000 to 115,000	33.6	28.9	20.8	83.3
115,000 to 80,000	45.2	37.1	20.8	103.1
80,000 to 70,000	94.9	45.4	21.8	163.1
70,000 to 57,000	64.8	32.0	22.8	119.6
57,000 to 40,000	100.3	59.4	22.8	182.5
40,000 to 25,000	99.5	54.4	22.8	176.7
25,000 to 13,000	143.5	74.5	22.8	240.8

Note: Total values for all sediment (including lutite) are estimated as a factor of 7.1 higher than those listed above. Values in 10^{11} grams per year.

I used late Würm flow-line reconstructions from Hughes and others (1977) to determine the area of each of the major ice sheets which those authors suggest supplied detritus to the North Atlantic. From their Figure 1, I calculate an area of 12.48×10^6 km^2. The masses of sediment deposited in the North Atlantic in the past 3 m.y. can be converted back to a volume of wet unconsolidated glacial marine drift by dividing by the dry weight/wet volume bulk density of 0.8 g/cm^3. This gives a total volume of 120,000 km^3 for the past 1.2 m.y. and probably more than 200,000 km^3 for the past 3 m.y. If this were spread across those parts of the ice sheets which fed detritus to the North Atlantic, it would form a layer of wet unconsolidated drift 16 m thick.

The roughly 350,000 km^3 of late Pliocene and Quaternary turbidite fill in the vast Sohm Abyssal Plain (Horn and others, 1972; Tucholke, Vogt, and others, 1975) emanated solely from eastern North America. These deep-sea deposits help explain the lack of thick drift deposits on eastern North America noted by Flint (1971). Together, they represent a layer of wet unconsolidated drift averaging in excess of 75 m removed from that part of North America east of the Laurentide ice divide.

Comparison to Other Oceans

Two parameters are necessary to compare total Pleistocene input of sand-sized detritus in the world's oceans: (1) the area in each ocean subject to ice-rafting, and (2) the mean glacial-interglacial input rate across each area. The existing data base in the other oceans is much smaller than in the North Atlantic; this comparison is thus admittedly very rough.

Antarctic Ocean estimates are based on Watkins and others (1974), Keany and others (1976), and Cooke (1976; 1977, personal commun.). The North Pacific values are based on data in Conolly and Ewing (1970), in Kent and others (1971), and in Robertson (1975) with additional inferences drawn from Griggs and Kulm (1969). Arctic Ocean calculations are based on data in Clark (1970, 1971) and Mullen and others (1972). Norwegian Sea estimates come from data in Kellogg (1975).

The regional extent of Pleistocene ice-rafting was determined from the source references listed above. The absolute input rates in specific cores were taken directly from the published calculations in two cases (Watkins and others, 1974; Keany and others, 1976); in other areas, the rates were calculated from the raw data. As discussed earlier, three quantities are needed to fix input rates in a given core: (1) mean sedimentation rates, from whatever stratigraphic control is available; (2) measurements of coarse-fraction noncarbonate percentages by weight; and (3) dry weight/wet volume bulk densities. The first two parameters were taken directly from the sources. Bulk densities of 0.8 g/cm^3 were assumed for all cores except in the North Pacific, where Robertson (1975) calculated 0.64 g/cm^3 as the best mean value.

I made calculations only for core intervals lying within the past 1.2 m.y., although not necessarily spanning that entire period. I also rejected cores spanning only a single glacial or interglacial part of the record as unrepresentative of long-term averages.

Only "deep-ocean" regions beyond the 100-fm contour were considered in the areal integrations. The rates determined from the published cores were regionally extrapolated across known (usually latitudinal) climatic zones. These calculated estimates are not meant to include the enormous thickness of detritus that may be deposited in deltas on the continental slope at the mouths of prominent ice streams. Only sand-fraction input (>62 μm) was calculated, because of its relatively unequivocal ice-rafted origin. The Antarctic sources had an upper size limit of 250 μm; this underemphasized the Antarctic rates somewhat relative to the North Atlantic. In the North Atlantic, sediment in the size fraction 250 to 2,000 μm constitutes about 7% by weight of the total noncarbonate sediment coarser than 62 μm. Subtracting it from the North Atlantic ice-rafted input would thus have minimal effect on the comparison. The Norwegian Sea analyses had no upper size

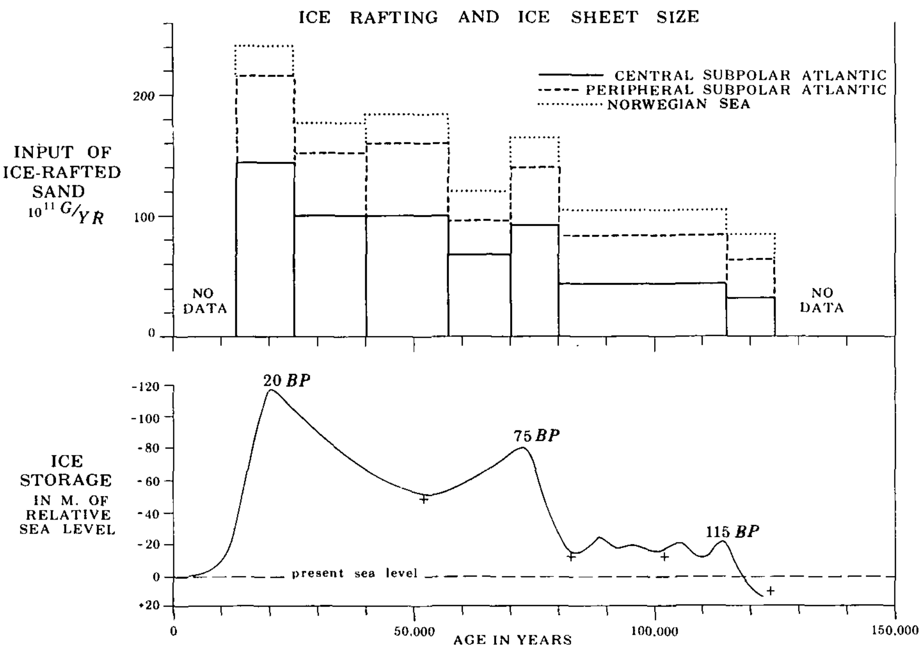

Figure 8. Total absolute input rate of ice-rafted sand during seven intervals mapped in Figure 4. Input integrated across central subpolar Atlantic outlined by heavy dashed line in Figure 1, peripheral subpolar Atlantic enclosed by dotted lines and continental slope in Figure 1, and Norwegian Sea (Fig. 5). Major increase of ice-rafting at 75,000 B.P. corresponds to southeastward shift in depositional pattern (Fig. 4). Lower curve showing isotopic evidence primarily of ice sheet growth (from Shackleton and Opdyke, 1973) matches ice-rafted changes.

TABLE 4. AREAL EXTENT OF HIGH-LATITUDE OCEANS AFFECTED BY ICE-RAFTING AND AVERAGE LATE QUARTERNARY INPUT OF SAND-SIZED DETRITUS IN EACH REGION

Ocean	Area (10^6 km^2)	Mean input rate across area (mg/cm^2/10^3yr)		Percentage of world total	
		All detritus	Nonvolcanic*	All detritus	Nonvolcanic*
North Atlantic	6.9	170	153	33	62
Norwegian Sea	2.2	100	90	6	12
Arctic	5.3	20	18	3	6
North Pacific	8.5	80	15	19	8
Antarctic	45.8	30	5	39	13

* Excluding ice-rafted or other volcanic input originating predominantly from ocean island sources.

cut-off; these rates must be somewhat overestimated relative to the Antarctic and North Atlantic.

Probably the greatest error in these rough calculations is the North Pacific Ocean estimate. This is based on cores located mostly in the west-central Pacific, leaving a large gap in the east near the Cordilleran source areas. Conolly and Ewing (1970) analyzed all detritus larger than 62 μm, while Kent and others (1971) and Robertson (1975) analyzed only for sand greater than 250 μm. Unpublished data from Kent (1977, personal commun.) were used to convert >250 μm input rates to >62 μm rates. By comparison with the other oceans, the Pacific estimates are particularly rough.

The rough ice-rafting calculations for all types of sand are listed in Table 4 (all detritus). With all detritus considered, the subpolar North Atlantic and circum-Antarctic share most (72%) of the world ice-rafted deposition. The rest is apportioned among the North Pacific, Norwegian Sea, and Arctic Ocean.

The ice-rafting estimates based on all detritus (Table 4) do not accurately portray what has been eroded from the continents by ice. Most of the North Pacific sand-sized detritus is volcanic debris, some of which was eroded from circum-Pacific Ocean islands (Conolly and Ewing, 1970). More than 80% of the sand-sized circum-Antarctic detritus is tephra erupted from the south Sandwich Islands onto passing sea and berg ice (Cooke, 1976; 1977, personal commun.) and deposited in the Atlantic Antarctic sector (long 70°W to 40°E). In the North Atlantic, about 10% of the sand-sized detritus comes from ocean islands, predominantly Iceland (Molnia, 1972).

To derive better estimates of the continental contributions, I used petrographic data from the source papers listed above to subtract the volcanic sand contribution that originated mainly from oceanic islands. The resulting input rates and estimates of percentage of world total (Table 4, nonvolcanic) show a strong dominance of the North Atlantic Ocean, which receives at latitudes south of Iceland roughly 62% of the world's ice-rafted nonvolcanic sand. The Norwegian Sea receives another 12%, which is almost equal to the entire circum-Antarctic continental deposition. About 6% is deposited in the Arctic, and about 8% in the North Pacific.

The largest surprise in these calculations is the low Southern Hemisphere nonvolcanic deposition. This cannot reflect ice passage through circum-Antarctic seas to deposition in lower latitudes, because the calculations cover both the glacial and interglacial depositional maxima (Watkins and others, 1974; Keany and others, 1976; Cooke, 1976). The data for the Antarctic Ocean require a very low ice-rafted input of continentally derived detritus for the Southern Ocean as a whole.

Despite deposition across an area six times larger than the subpolar North Atlantic, the total input of continental detritus is five times smaller, because the nonvolcanic input rates are 30 times lower. Input rates are low in part because Antarctica is a polar desert with very low precipitation except in fringing mountains. As a result, throughput of ice (considered as an erosional agent) may be slow and volumetrically less than in the cyclical Northern Hemisphere ice masses, which were of comparable total size but probably fed by more abundant moisture sources. Also, ice cover on Antarctica has been relatively constant through the past 1.2 m.y., largely prohibiting the various kinds of subaerial weathering that can provide continental detritus to ice sheets with fluctuating lateral limits.

In the Northern Hemisphere, the low Arctic Ocean value is easily explained; the permanent ice cover allows little melting. Similarly, the Norwegian Sea value is lower than the North Atlantic because prevalent glacial ice cover (particularly in the northwest) allows the ice to pass to lower latitudes without much melting.

The North Pacific contribution of nonvolcanic sand to the world total is minor (Table 4, nonvolcanic) partly because of the relatively small regions of continent that could have acted as detrital sources. The Bering Straits and frequently emergent Beringea land bridge cut off iceberg access from the Arctic Ocean to the North Pacific. The only viable iceberg sources were the western part of the Cordilleran ice, glaciated regions of the Aleutian arc, and areas of relatively minor glaciation in Kamchatka. The late Würm reconstruction of Hughes and others (1977) shows that the Cordilleran ice area draining into the Pacific was only 20% of that to the Atlantic. In addition, much of the detritus from the continents marginal to the North Pacific is volcanic; the nonvolcanic estimates in Table 4 must thus underestimate the true continental contribution.

In summary, the subpolar North Atlantic appears to be the dominant repository of ice-rafted continental detritus among the world's oceans. Northern Hemisphere oceans receive almost 90% of all ice-rafted nonvolcanic sand, and the subpolar North Atlantic receives about three-fourths of the Northern Hemisphere total.

ACKNOWLEDGMENTS

I thank K. Hanel, M. Prout, L. Glover, V. Kolla, and D. Cooke for running innumerable insoluble residue analyses; A. McIntyre, J. Sblendorio-Levy, and J. Durazzi for use of their coarse-fraction noncarbonate analyses of the V30 cores south of lat 45°N; G. Garner, C. Fruik, and D. Gross for general laboratory assistance; and M. Prout for computor processing of the data. This research was directly supported by National Science Foundation Grants GA-14177 and OCE75-18297. Office of Naval Research Grant N000-14-67-1A-0108-0004 and National Science Foundation Grants GA-10635 and GA-19690 to the Lamont-Doherty Geological Observatory Core Laboratory of Columbia University also aided our efforts. Most of the work was completed when I was employed by the U.S. Naval Oceanographic Office.

REFERENCES CITED

Berger, W. H., and Gardner, J. V., 1975, On the determination of Pleistocene temperatures from planktonic Foraminifera: Jour Foram. Research, v. 5, p. 102–113.

Berggren, W. A., 1972, Late Pliocene–Pleistocene glaciation, *in* Laughton, A. S., Berggren, W. A., and others, Initial reports of the Deep-Sea Drilling Project, Vol. 12: Washington, D.C., U.S. Govt. Printing Office, p. 953–963.

Bramlette, M. N., and Bradley, W. H., 1941, Lithology and geological interpretations: Geology and biology of North Atlantic deep-sea cores: U.S. Geol. Survey Prof. Paper 196, p. 1–34.

Broecker, W. S., and Ku, T. L., 1969, Caribbean cores P6304-8 and P6304-9: New analysis of absolute chronology: Science, v. 166, p. 404–406.

Broecker, W. S., and van Donk, J., 1970, Insolation changes, ice volumes, and the O^{18} record in deep-sea cores: Rev. Geophysics and Space Physics, v. 8, p. 169–198.

Clark, D. L., 1970, Magnetic reversals and sedimentation rates in the Arctic Ocean: Geol. Soc. America Bull., v. 81, p. 3129–3134.

——1971, Arctic Ocean ice cover and its late Cenozoic history: Geol. Soc. America Bull., v. 82, p. 3313–3324.

Conolly, J. R., and Ewing, M., 1965, Pleistocene glacial marine zones in North Atlantic deep-sea sediments: Nature, v. 208, p. 135–139.

——1970, Ice-rafted detritus in northwest Pacific deep-sea sediments, *in* Hays, J. D., ed., Geological investigations of the North Pacific: Geol. Soc. America Mem. 126, p. 219–231.

Cooke, D. W., 1976, Glacial-interglacial sedimentation changes in the Antarctic Ocean: Geol. Soc. America Abs. with Programs, v. 8, p. 820.

Emiliani, C., 1955, Pleistocene temperatures: Jour. Geology, v. 63, p. 538–578.

——1966, Paleotemperature analysis of the Caribbean cores P6304-8 and P6304-9 and a generalized temperature curve for the past 425,000 years: Jour. Geology, v. 74, p. 109–126.

Flint, R. F., 1943, Growth of North American ice sheet during the Wisconsin age: Geol. Soc. America Bull., v. 54, p. 325–362.
——1971, Glacial and Quaternary geology: New York, John Wiley & Sons, Inc., 892 p.
Griggs, G. B., and Kulm, L. D., 1969, Glacial marine sediments from the northeast Pacific: Jour. Sed. Petrology, v. 39, p. 1142–1148.
Hecht, A., 1973, A model for determining Pleistocene paleotemperatures from planktonic foraminiferal assemblages: Micropaleontology, v. 19, p. 68–77.
Holtedahl, H., 1955, On the Norwegian continental terrace, primarily outside Møre-Romsdal: Its geomorphology and sediments: Bergen Univ. Arb., v. 14, p. 1–209.
——1959, Geology and paleontology of Norwegian Sea bottom cores: Jour. Sed. Petrology, v. 29, p. 16–29.
Horn, D. R., Ewing, J. I., and Ewing, M., 1972, Graded-bed sequences emplaced by turbidity currents north of 20°N in the Pacific, Atlantic, and Mediterranean: Sedimentology, v. 18, p 247–275.
Hughes, T., Denton, G. H., and Grosswald, M. G., 1977, Was there a late-Würm Arctic ice sheet?: Nature, v. 266, p. 596–602.
Imbrie, J., and Kipp, N. G., 1971, A new micropaleontological method for quantitative paleoclimatology: application to a late Pleistocene Caribbean core, *in* Turekian, K., ed., The Late Cenozoic glacial ages: New Haven, Conn., Yale Univ. Press, p. 71–182.
Ives, J. D., Andrews, J. T., and Barry, R. G., 1975, Growth and decay of the Laurentide ice sheet and comparisons with Fenno-Scandinavia: Naturwissenschaften, v. 62, p. 118–125.
Keany, J., Ledbetter, M., Watkins, N., and Huang, T. C., 1976, Diachronous deposition of ice-rafted debris in sub-Antarctic deep-sea sediments: Geol. Soc. America Bull., v. 87, p. 873–882.
Kellogg, T. B., 1975, Late Quaternary climatic changes in the Norwegian and Greenland Seas, *in* Weller, G., and Bowling, S. A., eds., Climate of the Arctic: Alaska Science Conf., 24th, Fairbanks, 1975, proc., p. 3–36.
Kent, D., Opdyke, N. D., and Ewing, M., 1971, Climatic change in the North Pacific using ice-rafted detritus as a climatic indicator: Geol. Soc. America Bull., v. 82, p. 2741–2754.
Ku, T. L., Bischoff, J. L., and Boersma, A., 1972, Age studies of Mid-Atlantic Ridge sediments near 40°N and 20°N: Deep-Sea Research, v. 19, p. 233–247.
Kudrass, H-R., 1973, Sedimentation am Kontinentalhang vor Portugal und Marokko im Spätpleistozän and Holozän: "Meteor" Forschungsergebrisse, v. 13, p. 1–63.
McIntyre, A., Ruddiman, W. F., and Jantzen, R., 1972, Southward penetrations of the North Atlantic polar front: Faunal and floral evidence of large-scale surface water mass movements over the last 225,000 years: Deep-Sea Research, v. 19, p. 61–77.
McIntyre, A., and Kipp, N. G., with Bé, A.W.H., Crowley, T., Gardner, J., Prell, W., and Ruddiman, W. F., 1976, Glacial North Atlantic 18,000 years ago: A CLIMAP reconstruction, *in* Cline, R. M., and Hays, J. D., eds., Investigation of late Quaternary paleoceanography and paleoclimatology: Geol. Soc. America Mem. 145, p. 43–76.
McIntyre, A., and CLIMAP project members, 1976, The surface of the ice-age earth: Science, v. 191, p. 1131–1137.
Mesolella, K. J., Matthews, R. K., Broecker, W. S., and Thurber, D. L., 1969, The astronomical theory of climate change, Barbados data: Jour. Geology, v. 77, p. 250–274.
Molnia, B. F., 1972, Pleistocene ice rafting in the North Atlantic Ocean [Ph.D. thesis]: Columbia, Univ. South Carolina, 103 p.
Mullen, R. E., Darby, D. A., and Clark, D. L., 1972, Significance of atmospheric dust and ice rafting for Arctic Ocean Sediment: Geol. Soc. America Bull., v. 83, p. 205–212.
Pratt, R. M., 1961, Erratic boulders from Great Meteor Seamount: Deep-Sea Research, v. 8, p. 152–153.
Robertson, J. H., 1975, Glacial to interglacial oceanographic changes in the Northwest Pacific, including a continuous record of the last 400,000 years [Ph.D. thesis]: New York, Columbia Univ., 355 p.
Ruddiman, W. F., and Bowles, F. A., 1976, Early interglacial bottom current sedimentation on the Reykjanes Ridge: Marine Geology, v. 21, p. 191–210.
Ruddiman, W. F., and Glover, L. K., 1972, Vertical mixing of ice-rafted volcanic ash in North Atlantic sediments: Geol. Soc. America Bull., v. 83, p. 2817–2836.
——1975, Subpolar North Atlantic circulation at 9300 yr BP: Faunal evidence: Quaternary Research, v. 5, p. 361–389.
Ruddiman, W. F., and McIntyre, A., 1973, Time-transgressive deglacial retreat of polar water from the North Atlantic: Quaternary Research, v. 3, p. 117–130.
——1976, Northeast Atlantic paleoclimatic changes over the last 600,000 years, *in* Cline, R. M., and Hays, J. D., eds., Investigation of late Quaternary paleoceanography and paleoclimatology: Geol. Soc. America Mem. 145, p. 111–146.
Sancetta, C., Imbrie, J., and Kipp, N. G., 1973, Climatic record of the past 130,000 years in North Atlantic deep-sea core V23-82: Correlation with the terrestrial record: Quaternary Research, v. 3, p. 110–116.
Shackleton, N. J., 1969, The last interglacial in the marine and terrestrial records: Royal Soc. [London]Proc., ser. B., v. 174, p. 135–154.
Shackleton, N. J., and Opdyke, N. D., 1973, Oxygen isotope and paleomagnetic stratigraphy of equatorial Pacific core V28-238: Oxygen isotope temperatures and ice volumes on a 10^5 year and 10^6 year scale: Quaternary Research, v. 3, p. 39–55.
Siesser, W. G., and Rogers, J., 1971, An investigation of the suitability of four methods used in routine carbonate analysis of marine sediments: Deep-Sea Research, v. 18, p. 135–139.
Tucholke, B., Vogt, P. R., and others, 1975, *Glomar Challenger* drills in the North Atlantic: Geotimes, v. 20, no. 12, p. 18–21.
U.S. Naval Oceanographic Office, 1968, Oceanographic atlas of the North Atlantic Ocean, III: Ice: U.S. Naval Oceanog. Office Pub. 700, 157 p.
Warncke, D. A., 1970, Glacial erosion, ice rafting, and glacial marine sediments: Antarctica and the Southern Ocean: Am. Jour. Sci., v. 269, p. 276–294.
Watkins, N., Keany, J., Ledbetter, M. T., and Huang, T-C., 1974, Antarctic glacial history from analyses of ice-rafted deposits in marine sediments: New model and initial tests: Science, v. 186, p. 533–536.

MANUSCRIPT RECEIVED BY THE SOCIETY OCTOBER 10, 1976
REVISED MANUSCRIPT RECEIVED JANUARY 20, 1977
MANUSCRIPT ACCEPTED MARCH 7, 1977
CONTRIBUTION NO. 2557, LAMONT-DOHERTY GEOLOGICAL OBSERVATORY

Printed in U.S.A.